Performance evaluation of empirical models for vented lean hydrogen explosions

Anubhav Sinha, Vendra C. Madhav Rao, Jennifer X. Wen[*]

School of Engineering, University of Warwick, Coventry CV4 7AL, UK

ABSTRACT

This paper aims to provide a comprehensive review of available empirical models for overpressures predictions of vented lean hydrogen explosions. Empirical models and standards are described briefly, with discussion on salient features of each model. Model predictions are then compared with the available experimental results on vented hydrogen explosions. First comparison is made for standards tests, with empty container and quiescent starting conditions. Comparisons are then made for realistic cases with obstacles and initial turbulent mixture. Recently, a large number of experiments are carried out with standard 20-foot container for the HySEA project. Results from these tests are also used for model comparison. Comments on accuracy of model predictions, their applicability and limitations are discussed.

A new model for vented hydrogen explosion is proposed. This model is based on external cloud formation, and explosion. Available experimental measurements of flame speed and vortex ring formation are used in formulation of this model. All assumptions and modelling procedure are explained in detail. The main advantage of this model is that it does not have any tuning parameter and the same set of equations is used for all conditions. Predictions using this model show a reasonably good match with experimental results.

© 2018 Hydrogen Energy Publications LLC. Published by Elsevier Ltd. All rights reserved.

Introduction

Vented explosion is an important technique to relieve pressure in industrial enclosures and low strength buildings. Vent panels are designed based on the allowable peak pressure inside a building. To investigate peak overpressure attained in an accidental scenario, experiments can be both expensive and time consuming, especially in case of larger enclosures. Computational studies are also employed in these investigations, but studying a realistic size enclosure involves prohibitively large computational costs. Moreover, due to the large range of length and time scales involved in the phenomenon of vented explosion, accurately predicting overpressures is a challenging task. Empirical engineering models provide a fast and convenient method to predict overpressure, and can give an acceptable level of accuracy without much effort. Previous studies on vented explosions have mostly focussed on hydrocarbon gaseous fuels (Bauwens et al. [1]), dust, and vapours formed from liquid fuels. Recently, there has been a surge in use of hydrogen as a clean fuel and installations using and storing hydrogen are expected to increase in future. The objective of this paper is to present a review of available empirical models for overpressure

predictions for hydrogen explosions, and provide recommendations of the suitability and applicability of them for various conditions. Further, a new phenomenological model is also proposed to predict overpressures in hydrogen deflagrations. Model formulations and major assumptions are explained in detail. Various physical processes observed in vented deflagrations are accounted for and included in the model formulation. Predictions from this new model are found to be in good agreement with the available experimental results. The model does not involve any tuneable constants or adjustable parameters and predictions are made following the same set of equations for all cases.

Section Empirical models for overpressure predictions begins with a brief description of empirical models and major assumptions used in them. Section Model predictions for overpressure shows the comparison of model predictions with experimental measurements. Section New engineering model gives formulation for a new model and explain its formulations and equations to be used. Predictions from this model are also compared with the experimental results and found to be in a reasonably good agreement.

Empirical models for overpressure predictions

Four models are discussed in this section. They include the statutory standards − (i) EN-14994 [2], (ii) NFPA-68 [3], and other empirical models (iii) FM Global model [1,4−6], and (iv) Molkov model [13].

EN-14994 model [2]

The EN-14994 model is a part of statutory norms across Europe. The latest version available for this model was published in 2007 [2]. This model is based on gas explosion constant K_G. K_G is defined as the maximum value of pressure rise per unit time in a standard vessel. It is to be noted that this vessel is closed from all sides and different from the vented enclosure environment where this model is applied. One of the objectives of defining K_G for a closed vessel is that it can be measured with good repeatability and for different gases by maintaining the standard conditions. This model is divided into three formulations − (i) for compact enclosures (L/D < 2), (ii) Elongated enclosures ($2 \leq$ L/D $\leq$ 10), (iii) pipe (L/D > 10). First two formulations which are applicable for enclosures are discussed here.

(i) **Compact Enclosure** − The vent area for a given maximum pressure can be calculated using the following equation:

$$A_v E_f = \left[\left\{ (0.1265 \ln(K_G) - 0.0567)p^{-0.5817} \right\} + \left\{ 0.1754 p^{-0.5722} (p_{stat} - 0.1 \, bar) \right\} \right] V^{2/3}$$

(2.1)

where A_v is the vent area of enclosure, E_f is the venting efficiency (E_f=1 is used for lighter vents considered in this study), p is the peak overpressure, p_{stat} is the static pressure, V is the volume of the enclosure. This equation is designed for

calculating required venting area for a known permissible overpressure. This equation can also be modified to calculate the peak overpressure produced with a given vent area, as is done in the present study. This formulation does not account for initial turbulence, presence of obstacles, stratified fuel distribution, higher initial pressure, and partially filled enclosure. It is also recommended to be used for mixtures with $K_G \leq 550$ bar m/s. K_G values for hydrogen used in this study are obtained from the experimental measurements of Holtappels et al. [33].

(ii) **Elongated Enclosure** − Three equations are proposed to calculate overpressure for this formulation, and the peak overpressure is taken to be the maximum of all three values.

$$p = p_{stat} + \frac{0.023 \cdot S_L K \cdot W \cdot (L/D)^{1/3}}{V^{1/3}}$$

(2.2)

$$p = 0.015 \, d \cdot K$$

(2.3)

$$p = 0.015 \, d \cdot K + 0.15$$

(2.4)

where S_L is the laminar burning velocity, K is the vent coefficient − ratio of vessel cross-sectional area and total vent area, W is the weight per unit area of vent panel, D is the enclosure diameter, L is the enclosure length, d can be defined as:

$$d = x/D$$

where x is the maximum possible distance between ignition location and vent area. The parameters are to be specified in SI units. Equation (2.3) is to be used for $p_{stat} \leq 0.06$ bar and equation (2.4) is to be used when $p_{stat} > 0.06$ bar.

NFPA-68 model [3]

This model by National Fire Protection Association is the American standard model. The latest version available was published in 2013 [3]. The formulation recommends two different methods to be used (i) for reduced overpressure ≤ 0.5 bar, (ii) for reduced overpressure > 0.5 bar.

(i) **For $p \leq 0.5$ bar** - The recommended minimum vent area can be calculated for cases with $p \leq 0.5$ bar by using:

$$A_v = \frac{A_s \, C}{\sqrt{p}}$$

where A_v is the vent area, A_s is the internal surface area of enclosure, p is the reduced overpressure, and parameter C can be estimated as:

$$C = \frac{S_L \, \lambda \, \rho_u}{2 \, G_u \, C_d} \left[\left(\frac{P_{max} + 1}{P_0 + 1} \right)^{1/\gamma_b} - 1 \right] (P_0 + 1)^{1/2}$$

(2.5)

where S_L is the burning velocity of the mixture, λ is a factor that accounts for turbulence and flame instabilities, ρ_u is the

unburnt mixture density, C_d is the discharge coefficient of the vent, G_u is the unburnt mixture sonic flow mass flux (G_u =230.1 kg/m^2-s for an initial temp of 200 °C), P_{max} is the maximum pressure that can develop in the enclosure by burning the same gas mixture, P_0 is the initial static pressure, γ_b is the ratio of specific heat of the burnt gases.

(ii) **For $p > 0.5$ bar** - The formulation for higher static pressure can be given as:

$$A_v = A_s \left[\frac{1 - \left(\frac{P+1}{P_{max}+1} \right)^{1/\gamma b}}{\left(\frac{P+1}{P_{max}+1} \right)^{1/\gamma b} - \delta} \right] \frac{S_L}{G_u} \frac{\rho_u}{C_d} \frac{\lambda}{} \tag{2.6}$$

where δ can be defined as:

$$\delta = \frac{\left(\frac{P_{stat}+1}{P_0+1} \right)^{1/\gamma b} - 1}{\left(\frac{P_{max}+1}{P_0+1} \right)^{1/\gamma b} - 1}$$

To calculate the required vent area, it is required to guess a starting value of area, calculate pressure from it, and then iterate until the guessed pressure matches with the allowed pressure. This iterative procedure makes this model relatively difficult to use compared to other models.

FM global model

The FM Global model [1,4–6] is based on several experimental studies on their 63.7 m^3 enclosure, consisting of tests on hydrogen, methane and propane. The same set of equations is applicable for all these gases. This model hypothesises that there are three different factors responsible for pressure rise inside an enclosure − (i) External explosion (P1), (ii) Flame-acoustic interaction (P2), (iii) Flame wrinkling caused by obstacles (P3). These factors are responsible for multiple peaks observed in pressure transient measurements. Peak pressures for these processes are calculated separately and the maximum of these three peaks is the resultant overall peak overpressure. The model builds on the theoretical derivations of [7,8] which describe the flame propagation inside enclosure, pressure rise due to volumetric expansion of burnt products and pressure loss due to venting. The final overpressure depends on the interplay of these processes. Various physical processes and fuel properties are considered. The equation to calculate overpressure is given as [11]:

$$\frac{p}{p_e} = \frac{p_e G}{A_v^{*2} + \frac{p_e^2 G}{(p_{cv} - p_e)}} + 1 \tag{2.7}$$

where p is the pressure inside the enclosure, p_e is the external pressure, p_{cv} is the constant volume explosion pressure, G is given by:

$$G = \left(\frac{\gamma+1}{2} \right)^{\frac{\gamma}{(\gamma-1)}} - 1$$

and A_v^* can be calculated using:

$$A_v^* = \frac{a_{cd} A_v}{S_u A_f (\sigma - 1)} \tag{2.8}$$

where S_u is the flame speed, A_f is the flame surface area, σ is the expansion ratio, A_v is the vent area, a_{cd} is a parameter given as:

$$a_{cd} = c_d \sqrt{\frac{RT_v}{M_v} \gamma \frac{\gamma+1}{2}}$$

where c_d is the discharge coefficient (c_d =0.61 is recommended), R is the universal gas constant, T_v and M_v are vented gas temperature and molecular weight respectively, and γ is the ratio of specific heat capacities for the vented gases. It is assumed that the vented gases consist 90% of burnt gases and 10% of unburnt gases, and vent gas properties are computed using their weighted average. Flame area is calculated based on simplified geometric assumptions. The flame-ball is assumed to be approximately spherical for central ignition and half-ellipsoidal shaped for back-wall ignition. This formulation is used to calculate P1, the pressure peak due to external cloud. External pressure p_e is given by

$$\frac{p_e}{p_0} - 1 = \frac{5\gamma(\sigma - 1)\sigma r_e S_u AR \sqrt{k_T a}}{u_s^2} \tag{2.9}$$

where p_0 is the ambient pressure, r_e is the external cloud radius, u_s is sonic speed in unburnt gases, AR is the aspect ratio of the enclosure. To account for increase in flame-front area due to Rayleigh-Taylor instability, the factors k_T and a are used. The recommended value of k_T is 6.4 for all experiments presented in this work (Buawens [11]). a accounts for the increase in flow speed as the flame exits the vent.

A closer examination of equations (2.7)–(2.9) reveals the significance of each of the three processes. A higher value of external explosion will have higher p_e and hence it will become dominant term for the overall peak pressure. Moreover, increase in burning velocity (S_u) due to flame-acoustic interaction is expected to give a higher peak pressure P2. Lastly, it is understood that the obstacles increase the burning rate by increasing the flame surface area (A_f) by wrinkling. So a larger A_f will result in the dominant contribution from the obstacles.

For estimating transient peak P2, the flame is assumed to approach the internal walls and 0.9 times the internal surface area is used as the flame surface area. The flame speed for acoustic peak (P2), the laminar flame speed is multiplied by an acoustic coefficient whose value is determined using best fit with the experimental data. The values used in the present study is in the range 1.29–3.1 [11]. For increase in A_f because of obstacles, a model by Dorofeev [9,10] is employed. This gives the third pressure transient P3. The original formulation of this model had some issues with containers having large L/D, but this issue has been addressed in a recent update [11]. For the present study, fuel properties to be used for this model are calculated using the GASEQ calculator [12]. For obtaining acoustic coefficient and k_T, some useful guidelines are also provided by Jallais and Kudriakov [34].

A simplified version of this model is also published recently [36]. It is based on worst scenario approximation and is majorly based on this basic model. The final equation for overpressure is simplified version of equation (2.7) and can be stated as:

$$\frac{p}{p_e} = \frac{p_e G}{A_v^{*2}} + 1$$

Other equations of the simplified model are mostly similar to the basic detailed model. However, the detailed model is used for the present study.

Molkov and Bragin model (2015)

This model [13] is based on a novel concept of turbulent Bradley number, and it is based on previous versions of the same model and several numerical studies by the author and his group on vented deflagrations [14–19]. Bradley number can be defines as:

$$Br = \frac{A_v}{V^{2/3}} \frac{c_u}{S_L(\sigma - 1)}$$

where A_v is the vent area, V is the enclosure volume, c_u is the speed of sound in unburnt gases, S_L is the laminar burning velocity, and σ is the expansion ratio. This is further used to define turbulent Bradley number:

$$Br_t = \frac{\sqrt{\sigma/\gamma}}{\sqrt[3]{36 \, \pi_0}} \frac{Br}{\chi/\mu}$$

where γ is the specific heat ratio for unburnt gases, $\pi_0 = 3.141$, (χ/μ) is the deflagration-outflow interaction (DOI) number, in which is χ the turbulence factor and is the μ discharge coefficient. The basic assumption of this model is that the turbulent Bradley number correlates with overpressure. Various experimental studies are used to get curve-fit for this correlation and two equations are proposed. First is the equation that gives the best-fit values with the experimental data:

$$p = 0.33 \, Br_t^{-1.3} \tag{2.10}$$

where p is the reduced overpressure. The second equation is intended to give a conservative estimate:

$$p = 0.86 \, Br_t^{-1.3} \tag{2.11}$$

However, in this study, results using the best-fit model are only given. To calculate overpressure using these equations, in addition to fuel properties, DOI number also needs to be calculated. DOI number can be estimated by multiplying factors from various processes:

$$\frac{\chi}{\mu} = \Xi_K \cdot \Xi_{LP} \cdot \Xi_{FR} \cdot \Xi_{u'} \cdot \Xi_{AR} \cdot \Xi_0 \tag{2.12}$$

where Ξ_K is the factor for turbulence generated by the flame-front, Ξ_{LP} is factor for leading point, Ξ_{FR} is the factor to account for the increase in flame-front area due to fractal nature of flame surface, $\Xi_{u'}$ is the factor to account for initial turbulence, Ξ_{AR} is the factor for aspect ratio of enclosure, Ξ_0 is the factor to account for increased wrinkling due to presence of obstacles. No theoretical foundation has been given for this formulation of the DOI number and it appears to be of empirical nature. However the authors mention to have used computational modelling to formulate this equation, no derivation or detailed explanation is available. They have, however, given complete formulations to calculate all factors used in equation (2.2), except for the factor for obstacles, Ξ_0. For this factor, lack of experimental data is cited as a reason and values are suggested for FM Global results. It is to be noted that these values are not calculated but suggested based on the best-fit obtained with the experimental results. As such it

becomes challenging to use this formulation for predictions of cases with obstacles. A useful extension of this model is also proposed recently [37] which deals with the case of stratified fuel distribution.

Model predictions for overpressure

Overpressure predictions from the above discussed models are compared with available experimental results. The experimental results used in this evaluation are from the studies of:

(i) Bauwens et al. [4].
(ii) Kumar [20].
(iii) Daubech et al. [21].
(iv) Kumar [22].
(v) Bauwens et al. [23].
(vi) Schiavetti and Carcassi [24].
(vii) Skjold et al. [25].
(viii) Daubech et al. [35].

The experimental results are divided into various sets depending upon the complexity of the experiments and their applicability in real accidental scenarios.

Standard experiments

These experiments are carried out in an empty enclosure, with uniformly mixed fuel and quiescent initial mixture. These simplified experiments are different from actual accidental scenarios but offer set of standard and simple experiments which can be used to test the applicability of empirical models. The main objective in these experiments is to characterize the effect of parametric variations of fuel composition, vent area, and ignition location. The experiments considered under this section are.

(i) Bauwens et al. [4].
(ii) Kumar [20].
(iii) Daubech et al. [21].
(iv) Daubech et al. [35].

Bauwens et al. [4] carried out experiments in their 63.7 m^3 cuboidal enclosure and tested the variation of hydrogen concentrations, vent areas, and ignition locations. They have also used obstacles to model realistic accidents. The cases with obstacles will be considered in section Presence of obstacles. Kumar [20] has used 120 m^3 cuboidal enclosure, and studied the variation of vent size, ignition location and hydrogen concentrations. Kumar [20] has used the largest enclosure considered in this study and the experiments have used very lean mixtures of hydrogen (6%–12%). Daubech et al. [21] have used two cylindrical enclosures of 1 m^3 and 10 m^3 volumes and have studied the effect of variation of hydrogen concentration in both the enclosures. Daubech et al. [35] also carried out experiments in a cuboidal 4 m^3 enclosure with a transparent front wall. They have visualized flame propagation and external cloud formation.

The comparison of model predictions and overpressure measurements for Bauwens et al. [4] is shown in Fig. 1. Three ignition locations used are marked in the figure — central ignition (C), back-wall ignition (BW) and forward —wall (FW) ignition. As observed, the EN-14994 and NFP-68 models are over-predicting the pressure for all data points. FM Global model and Molkov model show reasonably good match. Molkov model is under-predicting for all back-wall ignition cases and over-predicting for all forward-wall ignition cases. This can be attributed to the model formulation, where ignition location is not accounted for. Fig. 2 shows comparison of model predictions with measurements of Kumar [20]. Different data points are marked for different ignition locations. Interestingly, EN-14994 model which over-predicted all data points for Bauwens et al. [4] is under-predicting some data points. These data points are for higher hydrogen concentrations. So, it can be inferred that EN-14994 model over-predicts for lower fuel concentrations and under-predicts for higher fuel concentrations. NFPA-68 is consistent with the trend shown in the previous example and is also over-predicting for all data points. FM Global model show significant under-predictions for many data points, and except for a

few points, all other points are under-predicted. Molkov model shows a large scatter, but shows a reasonable accuracy for many data points. It is to be noted that this data set is for very low hydrogen concentrations (6%—12%), and enclosure with high L/D [20]. Hence, it can be inferred that the Molkov model is most suitable in such conditions.

Fig. 3 shows comparison of model predictions with measurements of Daubech et al. [21]. The experiments are carried out at cylindrical enclosures with high L/D ratio. Data from different enclosures are shown in different symbols. The EN-14994 model over-predicts for lower hydrogen concentrations and under-predicts for higher hydrogen concentrations (around 20% and above). NFPA-68 over-predicts for most data points, but is seen to under-predict for hydrogen concentration of 10%—20% in both the enclosures. Similar trend is shown by FM Global model which under-predicts for approximately same fuel concentrations. Molkov model under-predicts for most data points. However, this model shows reasonable accuracy, and most of the predictions are close to experimental measurements.

Fig. 4 shows the predictions for experiments of Daubech et al. [35]. EN-14994 and Molkov model show under-
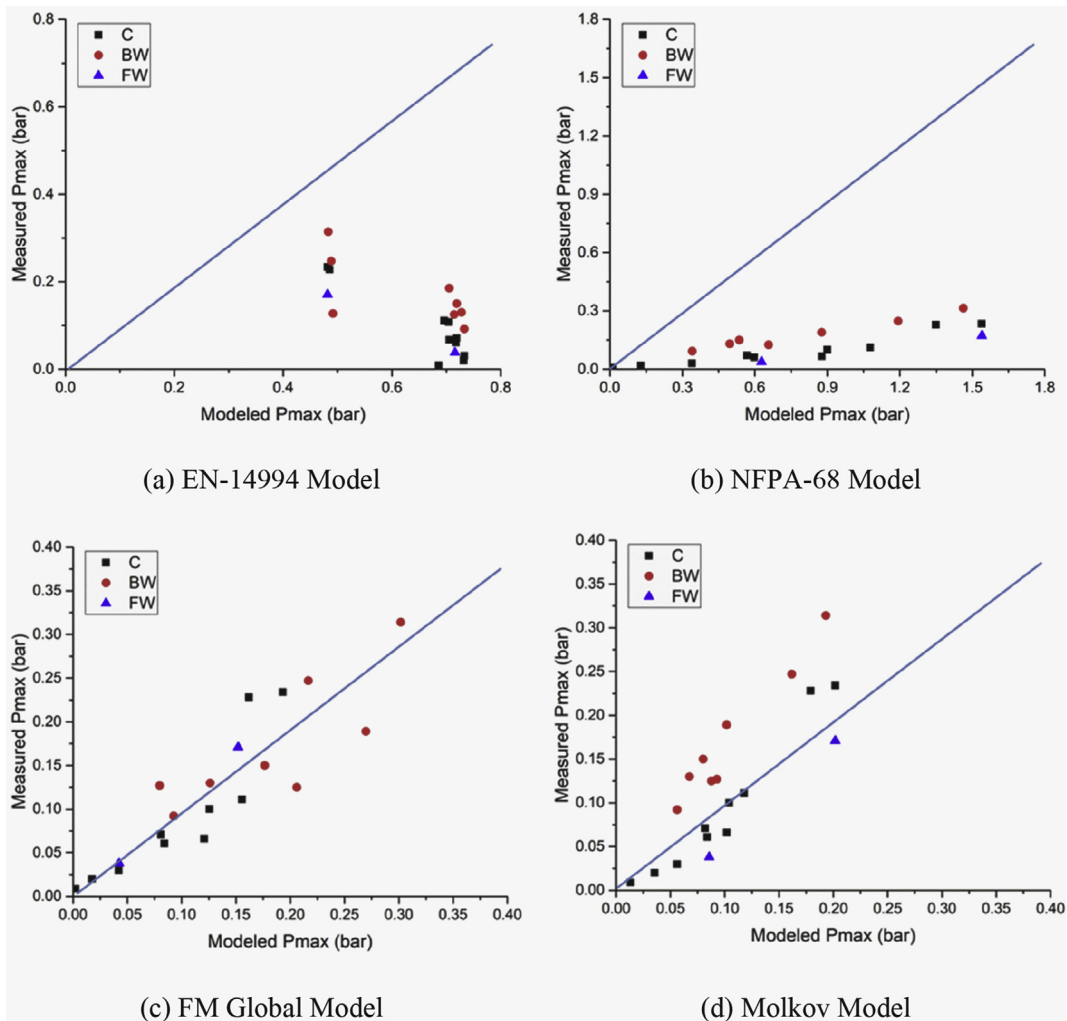

(a) EN-14994 Model

(b) NFPA-68 Model

(c) FM Global Model

(d) Molkov Model

Fig. 1 — Model predictions for experiments of Bauwens et al. [4] compared with experimental results.

(a) EN-14994 Model

(b) NFPA-68 Model
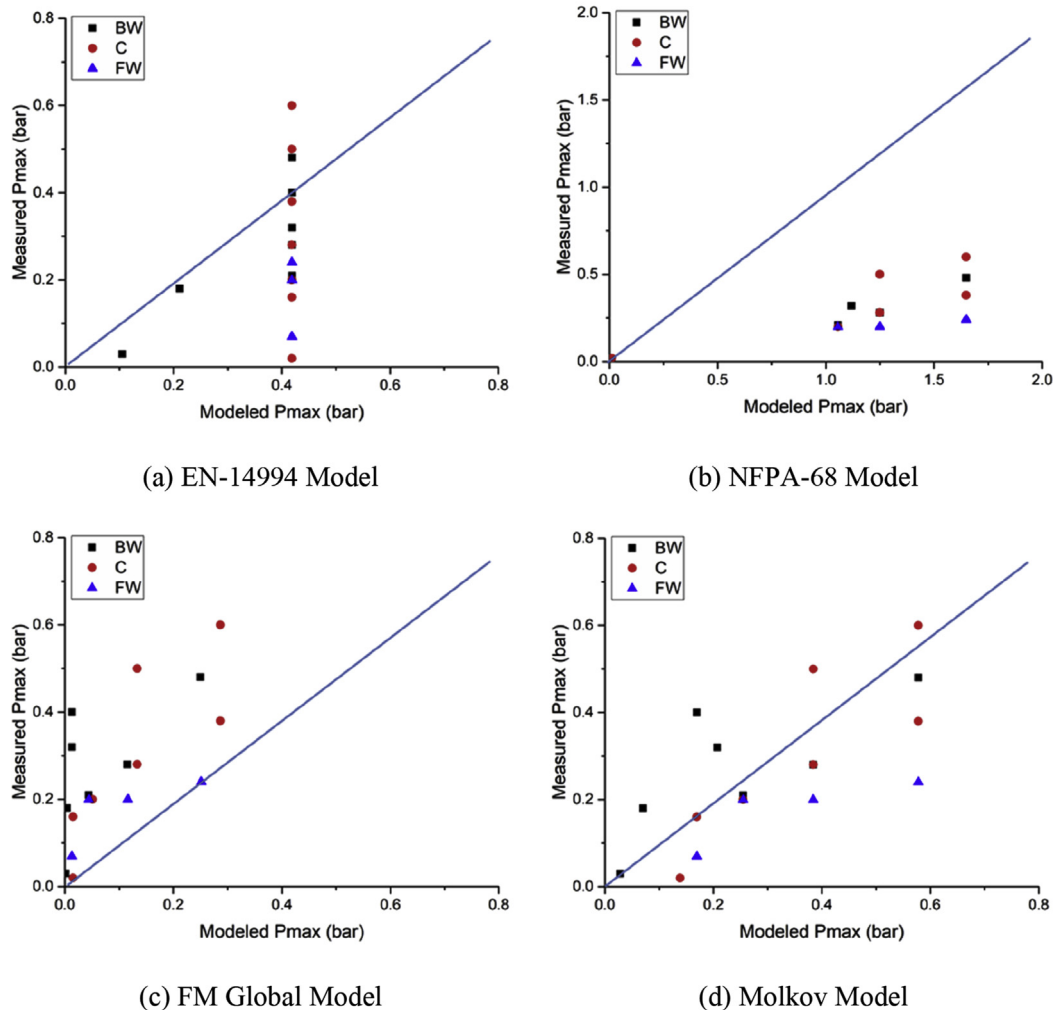
(c) FM Global Model

(d) Molkov Model

Fig. 2 – Model predictions for experiments of Kumar [20] compared with experimental results.

predictions for most data points. Though, a few points with lower hydrogen concentrations and lower overpressure are over-predicted. NFPA-68 and FM Global model over-predict for this set of experiments. The degree of over-prediction is higher for NFPA-68, and FM Global model appears to be the most preferred model for this configuration.

Presence of initial turbulence

In this section, cases where turbulence is generated in the unburnt mixture are considered. In an actual installation, accidents are caused by leaking gases, which are expected to promote turbulence. Hence these cases represent a more realistic accidental scenario as compared to cases considered in previous section (Standard experiments). Two studies considered here are –

(i) Kumar [22].
(ii) Bauwens et al. [23].

These investigations are carried on the same 120 m^3 (Kumar [22]) and 63.7 m^3 (Bauwens et al. [23]) enclosures used in previous studies discussed in section Standard

experiments. The only difference is that in these set of experiments, fans are installed inside the enclosures and the initial flow field is made turbulent before the mixture is ignited. The turbulent fluctuations (*u'*) are measured to be 1 m/s for Kumar's [22] study, while for Bauwens tests [22] *u'* vary from 0.09 m/s to 0.5 m/s for various experiments. EN-14994 and NFPA-68 models do not account for initial turbulence and hence only FM Global and Molkov's model will be used in subsequent discussion.

Fig. 5 shows the comparison of results from Kumar [22] with predictions from FM Global model and Molkov model. Kumar [22] has used different vent areas which are shown by different symbols. It is observed that both these models are under-predicting for almost all conditions. However, the predictions are in reasonable agreement with the measurements. Molkov model is observed to give slightly more accurate results than the FM Global model. Fig. 6 shows comparison for data from Bauwens et al. [23] with predictions from these models. It can be seen that the FM Global model shows a good agreement, while the Molkov model shows several over-predictions for all data points. It seems that the FM Global model should be preferred for the cases with initial turbulence.
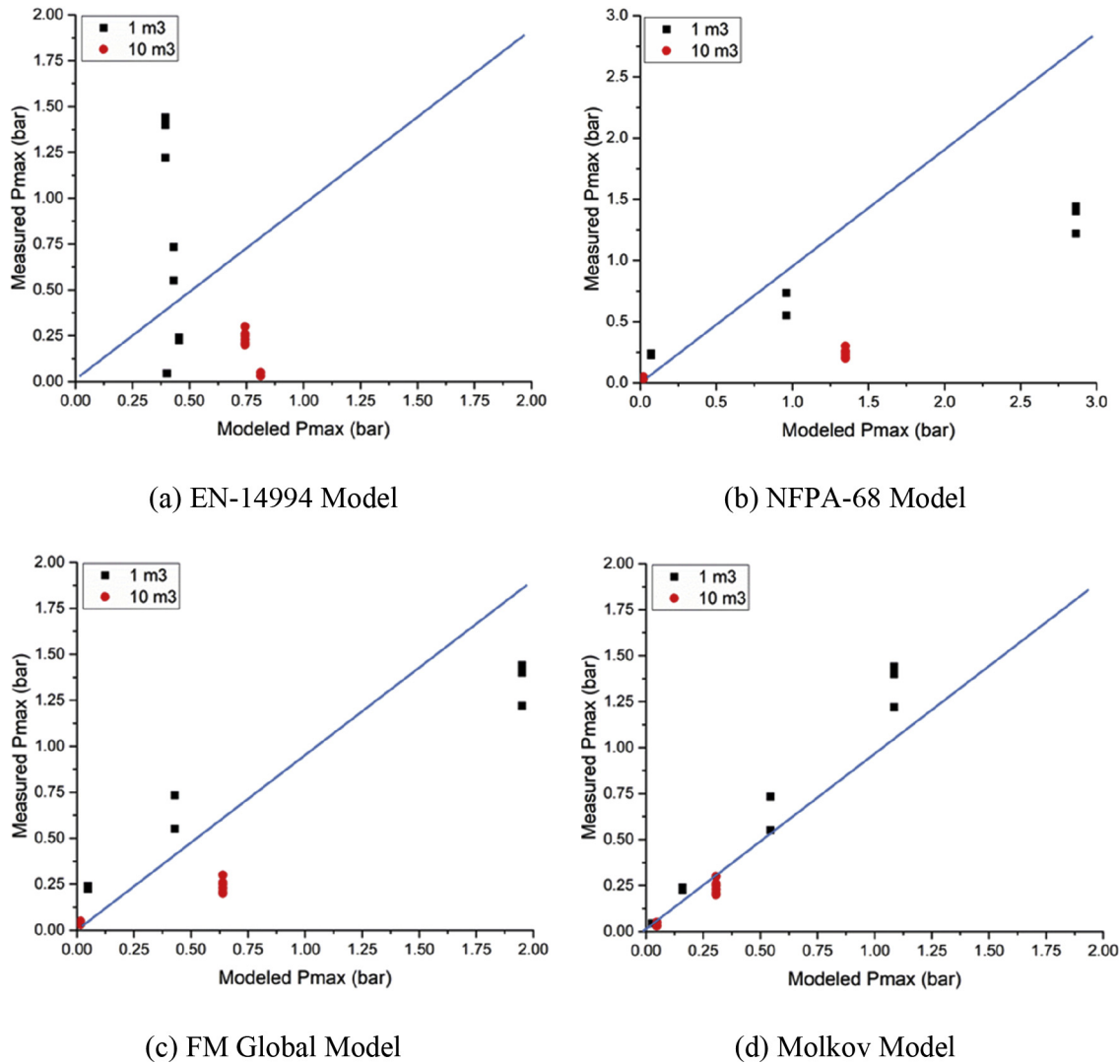
(a) EN-14994 Model

(b) NFPA-68 Model

(c) FM Global Model

(d) Molkov Model

Fig. 3 – Model predictions for experiments of Daubech et al. [21] compared with experimental results.

Presence of obstacles

In actual installations, the enclosures and buildings are expected to contain other equipment, pipes and structural parts which act as obstacles in flame-path. Hence these cases represent accidental scenario more closely. Experimental studies considered in this section are:

(i) Bauwens et al. [4].
(ii) Schiavetti and Carcassi [24].
(iii) Skjold et al. [25].

Fig. 7 shows predictions for results from Bauwens et al. [4] containing obstacles. Both the ignition locations used in experiments are shown with different symbols. As evident, both the models are giving reasonably accurate predictions. It is to be noted that while the FM Global model provide a complete formulation to account for obstacles, Molkov model provides a tuneable constant (Ξ_0), whose best-fit value has to be used. Values of Ξ_0 used here are 3.5 for back-wall ignition and 1 for

central ignition case. A modification of Molkov model to include proper formulation of this constant will make this model very useful for practical accidental scenarios.

Schiavetti and Carcassi [24] carried out a systematic study to assess the effect of different obstacle configuration on overpressure. Comparison for their results and corresponding predictions are shown in Fig. 8. $\Xi_0 = 2$ is used in Molkov model for all data points shown in Fig. 8. Both the models show large scatter in predictions. Generally, for experiments with obstacles, standard cylinders with circular or square cross sections are used. For these experiments Schiavetti and Carcassi [24] have used flat plates which have different recirculation regions than the standard cylinders. This different behaviour of flat plates can possibly be related to the large scatter in these predictions. It also highlights the fact that fundamental physics of the flow-field need to be accounted for to get reasonable predictions in realistic accidental scenarios.
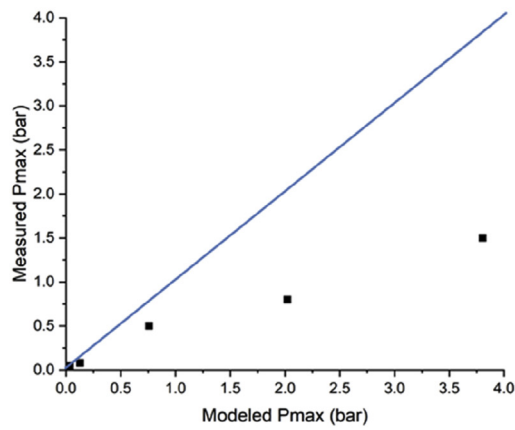
It is evident that most previous experimental investigations focussed on standard conditions with empty enclosures and quiescent mixture. To address the need for
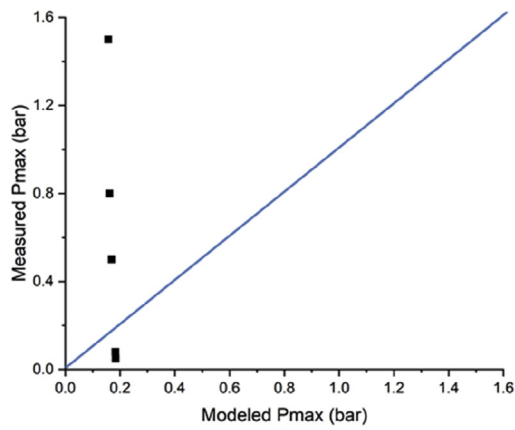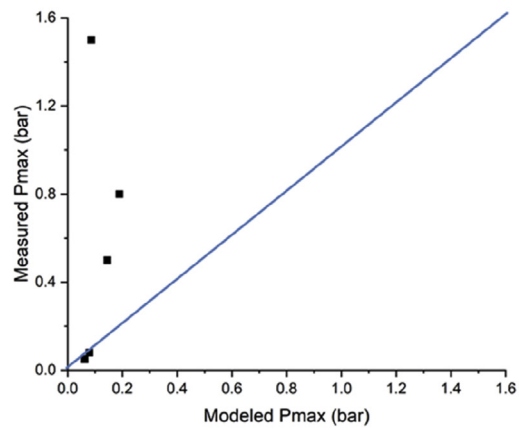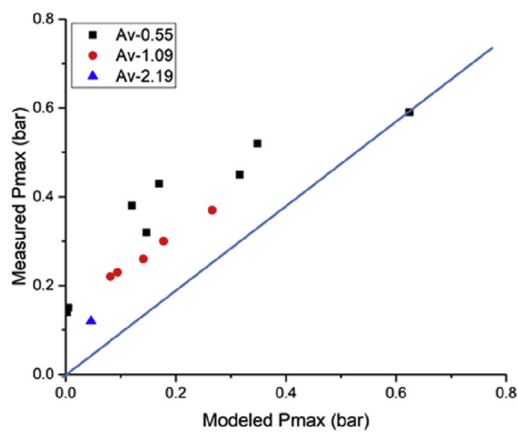
(a) EN-14994 Model
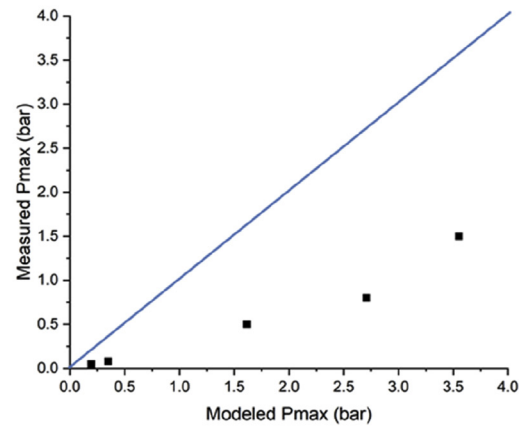
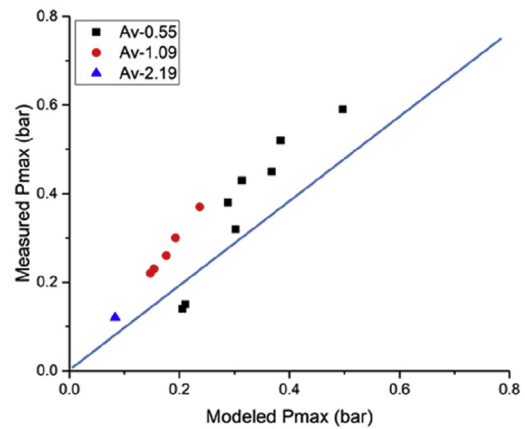(b) NFPA-68 Model

(c) FM Global Model

(d) Molkov Model

Fig. 4 − Model predictions for experiments of Daubech et al. [35] compared with experimental results.

(a) FM Global Model

(b) Molkov Model

Fig. 5 − Model predictions for experiments of Kumar [22] compared with experimental results.
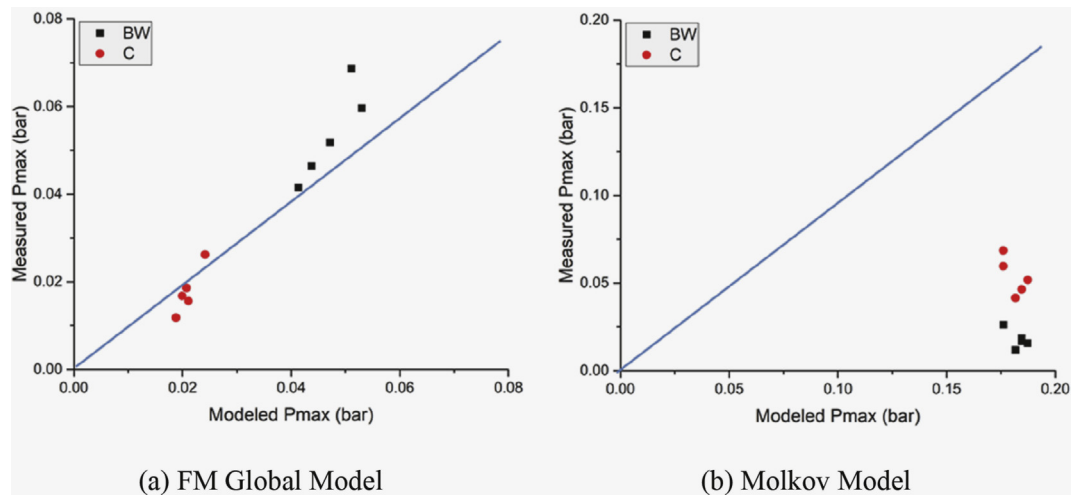
(a) FM Global Model　　　(b) Molkov Model

Fig. 6 – Model predictions for experiments of Bauwens et al. [23] compared with experimental results.
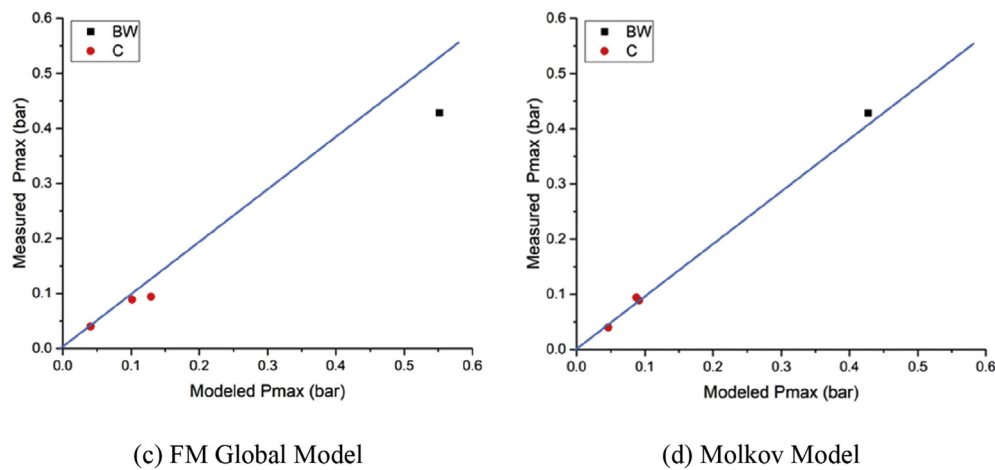

(c) FM Global Model　　　(d) Molkov Model

Fig. 7 – Model predictions for experiments of Bauwens et al. [4] with obstacles compared with experimental results.
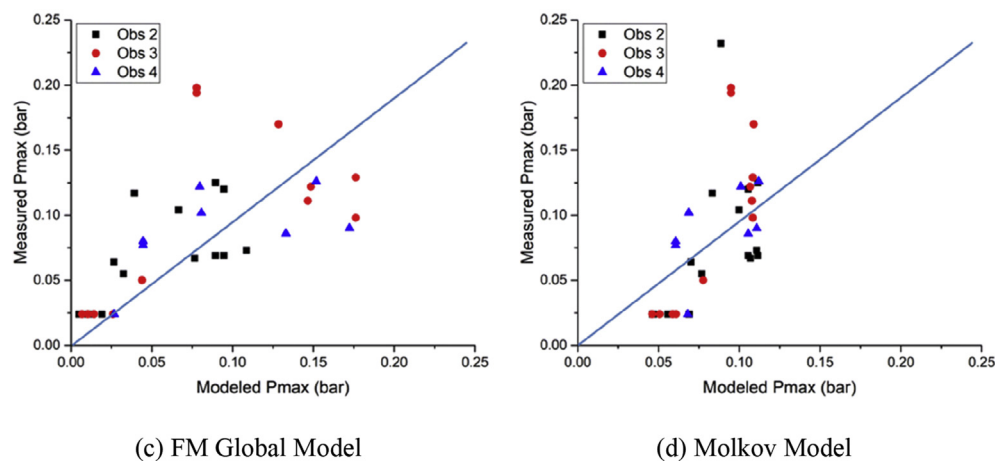

(c) FM Global Model　　　(d) Molkov Model

Fig. 8 – Model predictions for experiments of Schiavetti and Carcassi [24] compared with experimental results.

studies focussing on practical accidental conditions, recent experiments were conducted under the HySEA project. Under this project Skjold et al. [25] have used 20-foot ISO containers and conducted several experiments which mimic practical

conditions with different model obstacles. They have also shown that covering vent area using commercial vent panels instead of plastic sheet results in slightly higher peak pressure values. They have used two configurations with the ISO
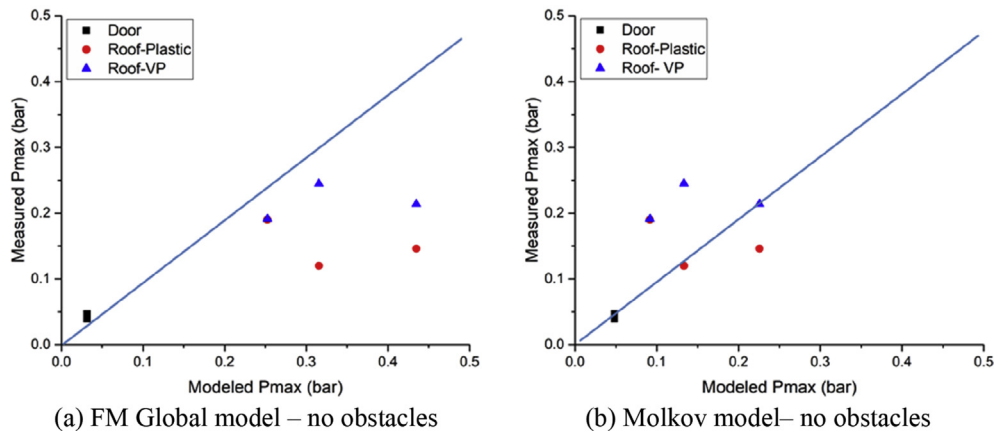
(a) FM Global model – no obstacles

(b) Molkov model– no obstacles

Fig. 9 – Model predictions for experiments of Skjold et al. [25] compared with experimental results.

containers - (i) venting through door, and (ii) venting through roof. They have used bottle basket and pipe rack as obstacles. More details about the experimental configuration can be found in Refs. [25,32]. Fig. 9 shows the predictions for cases with empty containers.

As evident, FM Global model shows slight under-prediction for door vented cases, and minor over-predictions for all roof-vented cases. Molkov model show similar scatter in roof-venting cases. Interestingly, it shows over-predictions for most roof-vented cases using plastic cover, while cases using commercial vent panel are under-predicted. Fig. 10 show predictions for cases with obstacles using FM Global model and Molkov model. A constant value of $\Xi_0 = 1.25$ is used for both bottle basket and pipe rack in Molkov model. In case where both bottle basket and pipe rack are used $\Xi_0 = 2.5$ is used. Fig. 10(a) and (b) show cases with door venting, and Fig. 10(c) and (d) show cases with roof venting. For door venting, almost all cases are over-predicted by FM Global model. The Molkov model shows good match at lower over-pressures, but for higher over-pressures Molkov model shows under-prediction. Similarly, for roof venting, FM Global model shows over-prediction for all data points; whereas Molkov model show under-prediction for most data points. It is to be noted that previous experiments Bauwens et al. [3] and Schiavetti and Carcassi [24] have used standard geometrical shapes as obstacles, whereas the HySEA experiments have used actual objects which are likely to be encountered in a gas storage facility. From the present analysis, it appears that the realistic obstacles are more challenging to include in engineering model and more experiments and modelling efforts are needed in this direction. In general, more experimental results are needed for realistic conditions which include – presence of obstacles, initial turbulence, stratified fuel distribution, multiple vents, etc.

New engineering model

Modelling details

As discussed in previous sections, and previous reviews [31], improvements in the existing models or a new model are required to predict for more realistic scenarios. Physical

processes involved in vented explosions should be accounted in the modelling efforts. This will help in modelling for new configurations and adding new features to the model, if required. The present section presents the formulation of a new model which attempts to model different physical processes in vented explosions. The vented deflagration phenomenon can be divided into several physical processes, which can be listed as:

(i) Ignition and spherical flame propagation
(ii) Venting of unburnt mixture and formation of the external cloud
(iii) Combustion of the external cloud producing external pressure
(iv) Internal flame generating overpressure

These processes can be modelled separately based on the underlying physical phenomenon, then the combinations of these sub-models can be used to compute the peak overpressure. The main advantage of formulating such a modular framework is that new features, like sub-models for obstacles and stratification can be added to the basic framework at a later stage without modifying other sub-models. Also, improvements in a particular part can be made without altering other sub-models. The modelling process can be explained in details as follows:

(i) **Ignition and spherical flame propagation** - The spherical flame propagation for hydrogen has been studied by several researchers. Recently, in a detailed study, Bauwens et al. [26] measured the spherical flame propagation in a 63.7 m^3 chamber and presented variation of flame propagation speed with radius using Background Oriented Schlieren (BOS) technique for various hydrogen concentrations. The results of this study will be used to model flame propagation. The flame propagation velocity with radius can be written as:

$$\frac{U}{U_0} = \left(\frac{R}{R_0}\right)^{\beta} \tag{4.1}$$

where U is the flame propagation velocity at radius R, U_0 is the flame propagation velocity at R_0, which is the critical radius

(a) FM Global Model – door venting,
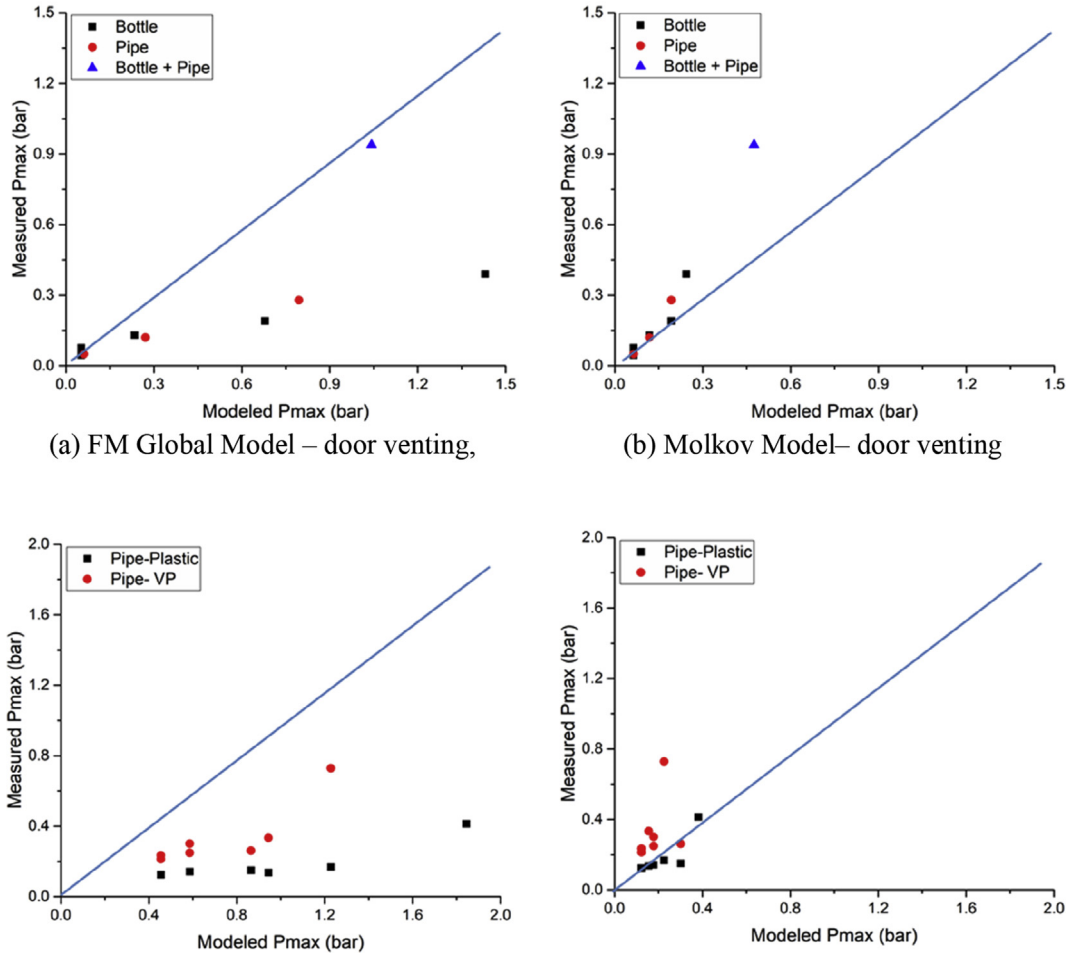

(b) Molkov Model– door venting

Fig. 10 – Model predictions for experiments of Skjold et al. [25] compared with experimental results – cases with obstacles.

for the onset of cellular instabilities, and β is fractal excess, experimentally observed to be constant at 0.243 for all hydrogen concentrations [26]. The values of U_0 and R_0 can be calculated using curve-fits to the experimental data [11,26].

$$U_0 = 0.0537\,x^2 - 1.008\,x + 5.5716 \quad (m/s)$$

$$R_0 = (1.4273\,x - 0.1942)/1000 \quad (m)$$

where x is the hydrogen concentration in percentage. Since:

$$U = \frac{dR}{dt}$$

Hence,

$$\frac{dR}{dt} = U_0\left(\frac{R}{R_0}\right)^\beta.$$

Rearranging and integrating

$$\int_0^R \frac{dR}{R^\beta} = \int_0^\tau \frac{U_0}{R_0{}^\beta}\,dt$$

$$\frac{R^{(1-\beta)}}{1-\beta} = \left(\frac{U_0}{R_0{}^\beta}\right)\tau \tag{4.2}$$

where, τ is the time taken by the flame to reach the radial position R. This equation can be used to calculate the time for the flame-front to reach the vent. The distance from the ignition source to the vent (R) can be estimated as:

$$R = \begin{cases} L & for\ Back-wall\ ignition \\ \dfrac{L}{2} & for\ Central-ignition \end{cases}$$

where L is the length of the enclosure. So, for a known L, time taken can be calculated as:

$$\tau = \left(\frac{R^{(1-\beta)}}{1-\beta}\right)\left(\frac{R_0{}^\beta}{U_0}\right) \tag{4.3}$$

and the flame-front velocity at that location can be calculated using equation (4.1).

(ii) **Venting of unburnt mixture and formation of the external cloud-** To study the external cloud, it is assumed that the enclosure acts like a piston-cylinder arrangement, where the flame-front pushing the gases work like a piston. The formation of external cloud by these vented gases is then calculated using the vortex ring theory given by Sullivan et al. [27]. The objective is to calculate the radius of the external cloud. To calculate the volume of the vented gases forming the cloud,
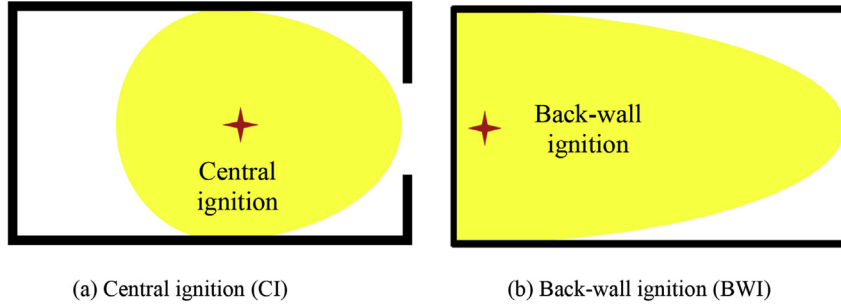
(a) Central ignition (CI)   (b) Back-wall ignition (BWI)

Fig. 11 – Schematic of the flame-shapes for different ignition locations.

the volume of the flame-ball inside the enclosure is required. Some simplifying assumptions for the flame shape are taken as: the flame-ball is considered to be a half ellipsoid for a Back wall ignition case and a sphere for a Central ignition case. The flame shape is shown in a schematic in Fig. 11.

The flame-ball volume for the Central-ignition case can be calculated as:

$$V_b = \left(\frac{4}{3}\pi R_{eq}{}^3\right) \tag{4.4}$$

where R_{eq} is the radius of the equivalent sphere.

$$R_{eq} = \frac{B+H}{4}$$

while for the Back-wall ignition case, the burnt volume can be estimated by calculating the volume of the semi-ellipsoid

$$V_b = \frac{\pi}{6}LBH \tag{4.5}$$

where L, B and H are the length, breadth and height of the enclosure, respectively. Finally, for both the cases, the volume of cloud can be calculated as:

$$V_c = V_b\left(1 - \frac{1}{\sigma}\right) \tag{4.6}$$

where V_c is the cloud volume, σ is the gas expansion ratio. Now, for the piston, the equivalent radius (R_0) can be calculated by equating the piston surface area to the vent area (A_v)

$$R_0 = \sqrt{\frac{A_v}{\pi}}$$

Piston stroke length using the cloud volume and equivalent piston area:

$$L_P = \frac{V_C}{A_V}$$

Saffman Vortex core size [27]:

$$a = \sqrt{4\,\nu\,\tau}$$

Radius of the vortex ring:

$$R_{Ring} = \sqrt[3]{\frac{3\,R_0^2\,L}{4\alpha}}$$

where, $\alpha = 1$

$$\wedge = \ln\left(\frac{8R_{Ring}}{a}\right) - 0.558$$

$$k = 0.65, \text{ and}$$

$$R_b = \sqrt[3]{\frac{9\,\pi\,R_0^2\,L_P}{4\alpha^2\wedge(1+k)}} \tag{4.7}$$

Radius of the external cloud is calculated using equation (4.7). More details about the cloud formation and comparison of experimentally measured cloud diameters and predictions from Equation (4.7) can be found in Ref. [28]. The cloud radius is further used to calculate overpressure generated by the external cloud combustion.

(iii) **Combustion of the external cloud and external pressure produced** –For external cloud combustion, the flame propagation velocity at cloud radius R_b can be obtained from equation (1). For pressure calculation, assuming Taylor's spherical piston theory [29], the Mach number at the cloud radius can be calculated as:

$$M_P = \frac{U_{cloud}}{a_0} \tag{4.8}$$

where M_P is the Mach number at the cloud boundary, U_{cloud} is the flame-speed at the cloud boundary, which can be calculated using equation (4.1) and cloud radius, a_0 is the speed of sound in unburnt gas mixture. The external pressure generated by this external cloud combustion can be estimated as:

$$P_{ex} = 2\gamma_u\left(1 - \frac{1}{\sigma}\right)\sigma^2\,M_P^2 \tag{4.9}$$

where γ_u is the ratio of specific heat of unburnt gases, and σ is the expansion ratio. This external pressure will be used for calculating pressure generated inside the enclosure, as described in the next section.

(iv) **Internal flame generating overpressure** - The fire-ball produced inside the enclosure can be approximated as standard geometrical shapes as explain in previous section. The flame area for those shapes can be calculated as:

$$A\,(sphere) = 4\pi R_{eq}^2$$

$$A(semi-ellipsoid) = 2\pi\left(\frac{(ab)^{1.6} + (bc)^{1.6} + (ca)^{1.6}}{3}\right)^{1/1.6}$$

(a) New model – Bauwens et al. data [3]

(b) New model-Bauwens et al. data [3]

(c) New model – Bauwens et al. data [3] with
different vent areas.

(d) New model – Bauwens et al. data [3] for
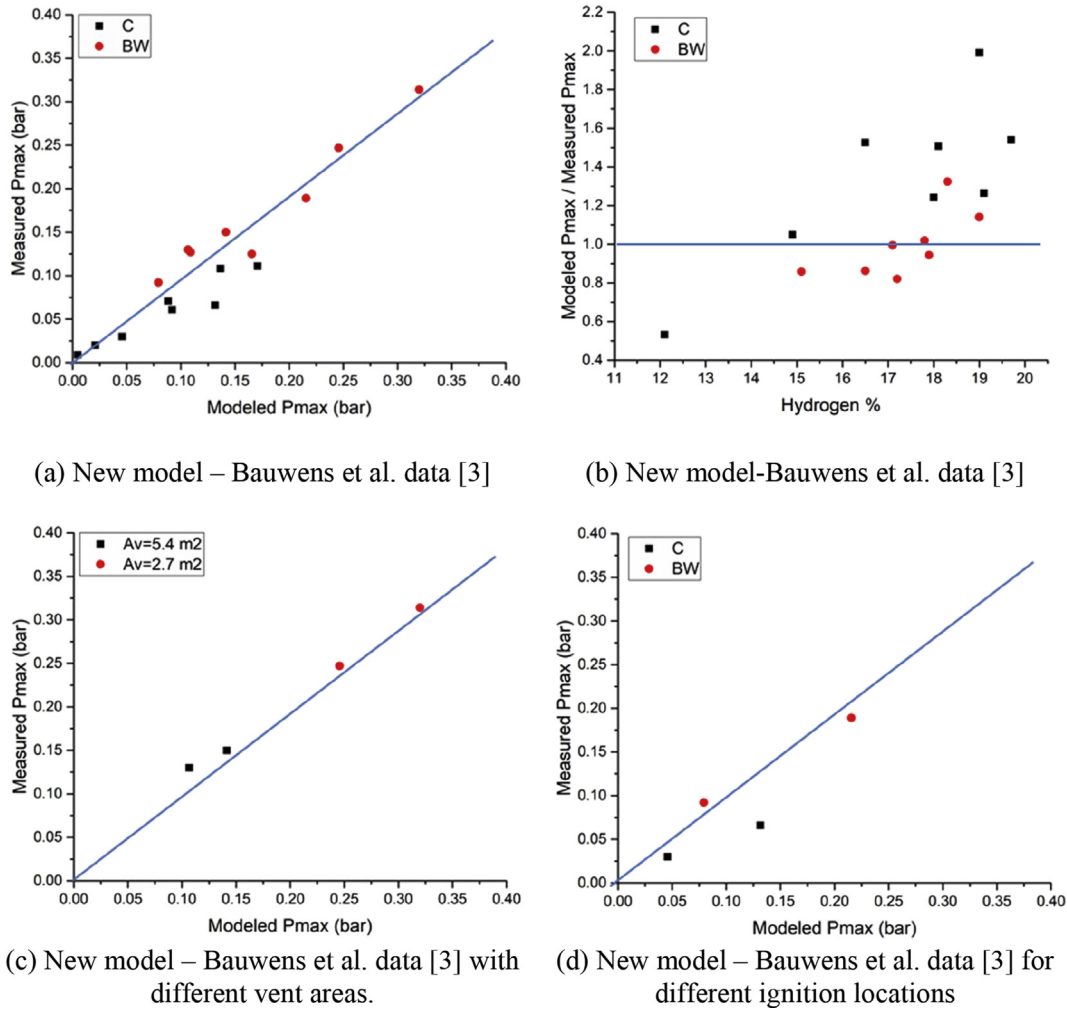different ignition locations

Fig. 12 — Overpressure predictions from the new model for Bauwens et al. data [3] (a) Comparison of the predictions with the measurements Bauwens et al. [3]; (b) Variation of the ratio between the of predicted and measured overpressure with hydrogen concentration; (c) Effect of vent size; (d) Effect of ignition location.

where $a=L$, $b=B/2$, and $c=H/2$. The volume of the burnt gases produced, can be calculated as:

$$\dot{V}_b = A_f \, U_f$$

where U_f is the flame propagation velocity calculated by equation (4.1). Also, the volume of the vented gases can be determined by Ref. [30]:

$$\dot{V}_v = u_{cd} \, A_v \sqrt{\frac{p - p_{ex}}{p_{cr} - p_{ex}}}$$

where u_{cd} can be calculated as [30]:

$$u_{cd} = C_d \sqrt{\frac{RT_v}{M_v} \, \gamma \frac{\gamma + 1}{2}}$$

where C_d is the coefficient of discharge with constant value of 0.6, R is the universal gas constant, T_v and M_v are the temperature and molecular weight of the vented gases, respectively. They are calculated assuming the vented gases are composed 90% of burnt gases and 10% of unburnt gases. The pressure inside the enclosure is controlled by two processes. It

increases with the generation of volume for the burnt gases while gas venting relieves this pressure. So, at the maximum over-pressure, the volumetric rate of gas venting will be equal to the volumetric rate of production of the burnt gases. Mathematically:

$$\dot{V}_b = \dot{V}_v$$

$$A_f \, U_f = u_{cd} \, A_v \sqrt{\frac{p - p_{ex}}{p_{cr} - p_{ex}}}$$

p is the pressure after solving these equations.

Comparison of new model predictions and experimental results

Model predictions from the new model are compared with experimental measurements of Bauwens et al. [3] in Fig. 12. Fig. 12(a) shows the comparison of measured and predicted overpressures. Fig. 12(b) shows the variation of the ratio of the predicted and measured overpressures with hydrogen
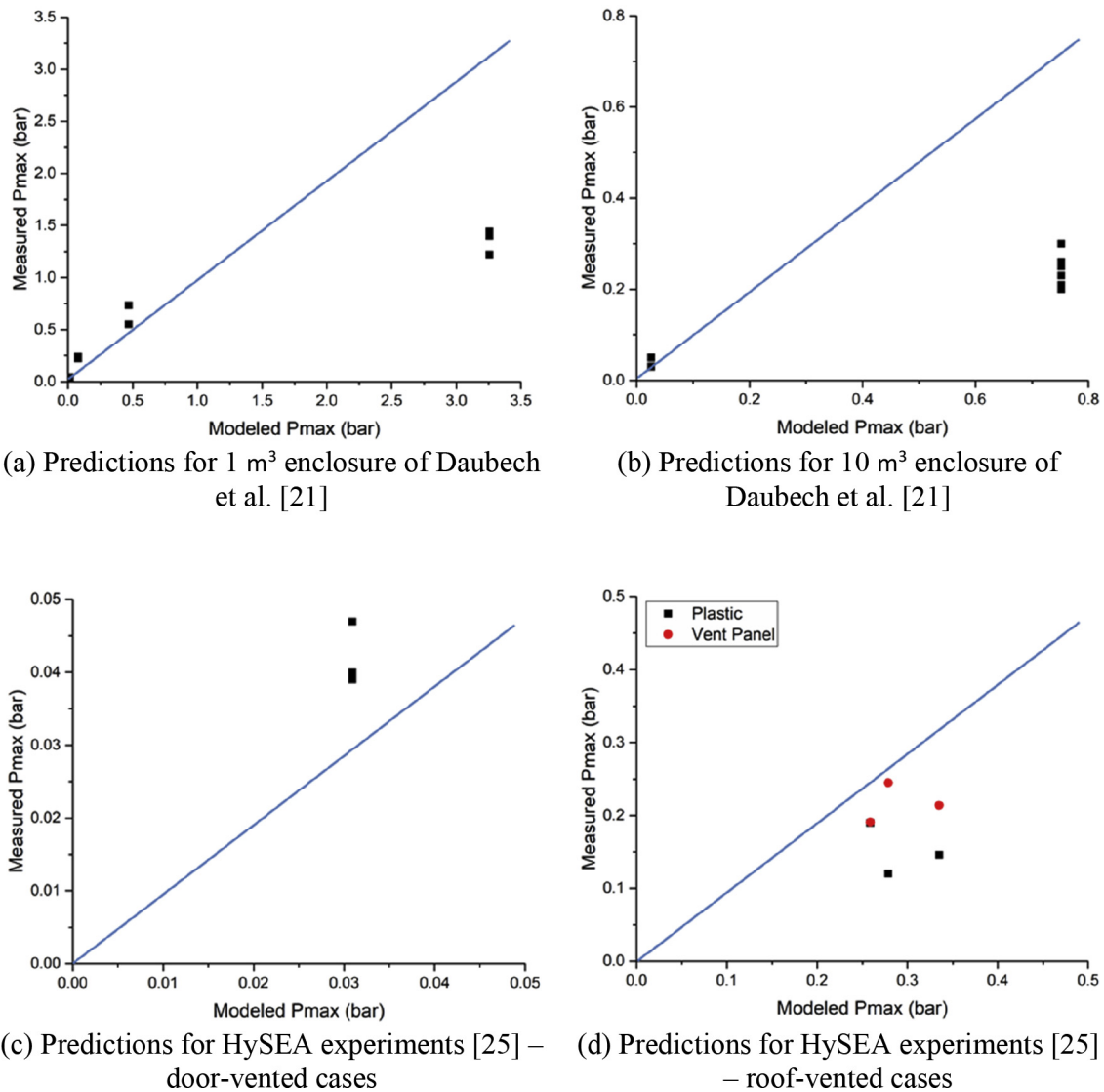
(a) Predictions for 1 m³ enclosure of Daubech et al. [21]

(b) Predictions for 10 m³ enclosure of Daubech et al. [21]

(c) Predictions for HySEA experiments [25] – door-vented cases

(d) Predictions for HySEA experiments [25] – roof-vented cases

Fig. 13 – **Overpressure predictions for experimental data from literature. Predictions for data from (a) 1 m³ enclosure Daubech et al. [21], (b) 10 m³ enclosure of Daubech et al. [21], (c) door-vented cases of Skjold et al. [25], (d) roof-vented cases of Skjold et al. [25].**

concentration. The new model shows more accurate predictions than other available models previously discussed (see Fig. 1). Also, there is no apparent bias towards any hydrogen concentration and predictions and the predictions are equally dispersed. Furthermore, the new model does not have any adjustable parameters that require fine tuning for each case, and the same procedure of calculation is followed for all studies. Fig. 12(c) and (d) also show that the effect of vent size and ignition location is well captured by the new model. In Fig. 12 (c), the two pair of points which show the increase in overpressure with decrease in vent area. This experimentally observed trend is well captured by the present model. Another parameter under investigation is the ignition location. It is experimentally observed that back-wall ignition produces higher overpressure as compared to central ignition for the same enclosure geometry and fuel composition. This effect is also captured by the present model as shown in Fig. 12(d).

Further, other experimental studies from literature are also used to test the overpressure predictions of the present model. Fig. 13 (a) and (b) show the predictions for the tests of Daubech et al. [21]. Also, predictions for 20-foot ISO container used in HySEA experiments are shown in Fig. 13 (c) and (d). The model is able to predict with reasonable accuracy for both configurations as well as for plastic cover and vent panel cover. The present model is able to give reasonable predictions for these experimental investigations which range from enclosure volume of 1 m³ to 63.7 m³ and hydrogen concentration of 10%–27%. It must be noted that the formulation of the present model described in this paper is focussed on the external pressure peak (P1) and is applicable to uniform fuel distribution and empty enclosures. The present formulation also does not account for initial turbulence in the enclosure. Hence, validation cases with obstacles and with initial turbulence are not shown in the present discussion. Further work is under

progress to incorporate formulation for all these sub-processes.

Conclusions

This paper presents a review of available empirical models and standards for predicting overpressure in accidental explosions. Model equations and major assumptions are briefly discussed, highlighting the salient features and major assumptions of each model. These models are then assessed by comparing their predictions with the available experimental data on vented hydrogen explosions. A large range of data set, comprising of enclosures ranging from 1 m³ to 120 m³ are considered. Recent experiments conducted on 20-foot ISO containers under the HySEA project are also used in this study. It is observed that EN-14994 model gives over-predictions for lower hydrogen concentrations and under-predictions for higher concentrations. NFPA-68 model is found to over-predict for most of data points considered in this study. Both FM Global and Molkov model are found to be reasonably accurate for overpressure predictions. However there are some issues with both of these models that need to be addressed for predictions of realistic accidental scenarios. For instance, the FM Global model is found to under-predict cases with initial turbulence, at lower hydrogen concentration, and for high L/D ratios. On the other hand, Molkov model needs a proper formulation for accounting for obstacles. Both these models show a large scatter in predictions for realistic obstacle used in recent studies [24,25].

A new model based on external cloud explosion is also proposed. This model shows better or comparable predictions with other models for available experimental data on lean hydrogen explosions. The major advantage of this model is that it accounts for various physical processes responsible for pressure rise, and gives a modular formulation. The use of modular formulation is that any new process can be incorporated independent of other processes. Another advantage of this model is that it does not have any adjustable parameters that require fine tuning for each case, and the same procedure of calculation is followed for all studies. Further development on this model is required to account for realistic accidental scenario of stratified fuel distribution and presence of obstacles.

Acknowledgements

REFERENCES

[1] Bauwens C Regis, Chaffee Jeff, Dorofeev Sergey. Effect of ignition location, vent size, and obstacles on vented explosion overpressures in propane-air mixtures. Combust Sci Technol 2010;182(11-12):1915–32.

[2] EN, BS. 14994: 2007. Gas explosion venting protective systems. 2007.

[3] NFPA 68. Standard on explosion protection by deflagration venting. 2013th ed. National Fire Protection Association; 2013.

[4] Bauwens CR, Chao J, Dorofeev SB. Effect of hydrogen concentration on vented explosion overpressures from lean hydrogen–air deflagrations. Int J Hydrogen Energy 2012;37(22):17599–605.

[5] Bauwens CR, Chao J, Dorofeev SB. Evaluation of a multi peak explosion vent sizing methodology IX ISHPMIE. In: International symposium on hazard, prevention and mitigation of industrial explosions; 2012.

[6] Chao J, Bauwens CR, Dorofeev SB. An analysis of peak overpressures in vented gaseous explosions. Proc Combust Inst 2011;33(2):2367–74.

[7] Bradley D, Mitcheson A. The venting of gaseous explosions in spherical vessels. Combust Flame 1978;32:221.

[8] Tamanini F. Characterization of mixture reactivity in vented explosion. In: 14th international colloquium on the dynamics of explosions and reactive systems, Coimbra, Portugal; 1993.

[9] Dorofeev SB. Flame speed correlation for unconfined gaseous explosions. Process Saf Prog 2007;26:140.

[10] Dorofeev SB. Evaluation of safety distances related to unconfined hydrogen explosions. Int J Hydrogen Energy 2007;32:2118.

[11] Bauwens CR. Personal communication. 2017.

[12] www.gaseq.co.uk.

[13] Molkov V, Bragin M. Hydrogen–air deflagrations: vent sizing correlation for low-strength equipment and buildings. Int J Hydrogen Energy 2015;40(2):1256–66.

[14] Molkov VV. Unified correlations for vent sizing of enclosures at atmospheric and elevated pressures. J Loss Prev Process Ind 2001;14(6):567–74.

[15] Molkov V, Dobashi R, Suzuki M, Hirano T. Modeling of vented hydrogen-air deflagrations and correlations for vent sizing. J Loss Prev Process Ind 1999;12(2):147–56.

[16] Keenan JJ, Makarov DV, Molkov VV. Rayleigh–Taylor instability: modelling and effect on coherent deflagrations. Int J Hydrogen Energy 2014;39(35):20467–73.

[17] Molkov VV. Theoretical generalization of international experimental data on vented explosion dynamics. In: Proceedings of the first international seminar on fire and explosion hazard of substances and venting of deflagrations, moscow; 1995.

[18] Molkov VV, Korolchenko A, Alexandrov S. Venting of deflagrations in buildings and equipment: universal correlation. Fire Saf Sci 1997;5:1249–60.

[19] Molkov, V. Fundamentals of hydrogen safety engineering, Part II, www.bookboon.com.

[20] Kumar K. Vented combustion of hydrogen-air mixtures in a large rectangular volume. In: 44th AIAA aerospace sciences meeting and exhibit; 2006.

[21] Daubech J, Proust C, Jamois D, Leprette E. Dynamics of vented hydrogen-air deflagrations. In: 4. International conference on hydrogen safety (ICHS 2011); 2011, September.

[22] Kumar RK. Vented turbulent combustion of hydrogen-air mixtures in A large rectangular volume. In: 47th AIAA aerospace sciences meeting; 2009. Paper AIAA 2009-1380.

[23] Bauwens CR, Dorofeev SB. Effect of initial turbulence on vented explosion overpressures from lean hydrogen–air deflagrations. Int J Hydrogen Energy 2014;39(35):20509–15.

[24] Schiavetti M, Carcassi M. Maximum overpressure vs. H2 concentration non-monotonic behavior in vented deflagration. Experimental results. Int J Hydrogen Energy 2017;42(11):7494–503.

[25] Skjold T, Hisken H, Lakshmipathy S, Atanga G, van Wingerden M, Olsen KL, et al. Vented hydrogen deflagrations in containers: effect of congestion for homogeneous mixtures. ICHS-2017; 2017.

[26] Bauwens CRL, Bergthorson JM, Dorofeev SB. Experimental investigation of spherical-flame acceleration in lean hydrogen-air mixtures. Int J Hydrogen Energy 2017;42(11):7691–7.

[27] Sullivan IS, Niemela JJ, Hershberger RE, Bolster D, Donnelly RJ. Dynamics of thin vortex rings. J Fluid Mech 2008;609:319–47.

[28] Sinha A, Wen JX. Phenomenological modelling of external cloud formation in vented explosions. In: SHPMIE-2018, Kansas, USA; Aug 2018.

[29] Strehlow RA, Luckritz RT, Adamczyk AA, Shimpi SA. The blast wave generated by spherical flames. Combust Flame 1979;35:297–310.

[30] Tamanini F. Characterization of mixture reactivity in vented explosion. In: 14th international colloquium on the dynamics of explosions and reactive systems; 1993.

[31] Sinha A, Vendra C, Rao Madhav, Wen JX. Evaluation of engineering models for vented lean hydrogen deflagrations. In: ICDERS 2017, Boston; 2017.

[32] Sinha A, Vendra C, Rao Madhav, Wen JX. Comparison of engineering and CFD model predictions for overpressures in vented explosions. In: ISHPMIE-2018, Kansas, USA; Aug 2018.

[33] Holtappels K, Liebner C, Schröder V, Schildberg HP. Report on experimentally determined explosion limits, explosion pressures and rates of explosion pressure rise-Part 1: methane, hydrogen and propylene; Contract No. EVG1-CT-2002-00072. 2006.

[34] Jallais S, Kudriakov S. An inter-comparison exercise on engineering models capabilities to simulate hydrogen vented explosions. Brussels: ICHS 2013; Sep. 2013.

[35] Daubech J, Proust C, Gentilhomme O, Jamois C, Mathieu L. Hydrogen-air vented explosions: new experimental data. In: 5th international conference on hydrogen safety, Brussels, Belgium; 2013, September.

[36] Bauwens CR, Dorofeev SB. A simplified approach to gas explosion vent sizing. In: American Institute of Chemical Engineers 2018 spring meeting and 14th global congress on process safety Orlando, Florida, April 2018; 2018.

[37] Makarov D, Hooker P, Kuznetsov M, Molkov V. Deflagrations of localised homogeneous and inhomogeneous hydrogen-air mixtures in enclosures. Int J Hydrogen Energy 2018;43(20):9848–69.